

Blue Spectra of Kalb-Ramond Axions and Fully Anisotropic String Cosmologies

Massimo Giovannini*

DAMTP, Silver Street, CB3 9EW Cambridge, United Kingdom
and

Institute of Cosmology, Department of Physics and Astronomy,
Tufts University, Medford, Massachusetts 02155, USA

The inhomogeneities associated with massless Kalb-Ramond axions can be amplified not only in isotropic (four-dimensional) string cosmological models but also in the fully anisotropic case. If the background geometry is isotropic, the axions (which are *not* part of the homogeneous background) develop, outside the horizon, growing modes leading, ultimately, to logarithmic energy spectra which are “red” in frequency and *increase* at large distance scales. We show that this conclusion can be evaded not only in the case of higher dimensional backgrounds with contracting internal dimensions but also in the case of string cosmological scenarios which are *completely anisotropic in four dimensions*. In this case the logarithmic energy spectra turn out to be “blue” in frequency and, consequently, *decreasing* at large distance scales. We elaborate on anisotropic dilaton-driven models and we argue that, incidentally, the background models leading to (or flat) logarithmic energy spectra for axionic fluctuations are likely to be isotropized by the effect of string tension corrections.

I. INTRODUCTION

In recent years a lot of effort has been devoted to the analysis of rather peculiar phenomenological implications of string inspired cosmological models [1]. One of the distinctive features of the low-energy string effective action is indeed the presence of the dilaton field whose sharp growth amplifies, via gravitational instability, not only the scalar and tensor fluctuations of the geometry [2] but also the (quantum mechanical) inhomogeneities associated with other fields which are not part of the homogeneous background like the gauge fields [3,4] and the universal axion of string theory [5,6], i.e. the (four-dimensional) dual of the Kalb-Ramond antisymmetric tensor field present in the (effective) low energy limit of the action.

The main difference between the amplification of the metric fluctuations and the amplification of other fields with no homogeneous background turned out to be, a posteriori, the spectral amplitudes. In the case of metric fluctuations the growing modes appearing in the corresponding evolution equations lead typically, to increasing (“violet”) spectra, whereas in the case of Abelian gauge fields and axions the spectral slope can be much milder.

These results refer to the case of a homogeneous background geometry whose spatial section naturally decomposes into the direct product of two (maximally symmetric) Euclidean sub-manifolds which will be called, for short, *external* and *internal*. This type of metric describes a situation of dimensional decoupling where the external dimensions expand and the internal dimensions contract¹. In previous studies concerning the phenomenological implications of string inspired scenarios, the expanding dimensions have been always taken to be isotropic (i.e. described by a unique scale factor). Similarly, the internal dimensions have been also taken to be isotropic (this situation can happen if we compactify the internal dimensions on a six-dimensional torus). This choice is not a limitation. In fact we know that the dilaton “vacuum” solutions can be solved for arbitrary (anisotropic) manifolds.

There are, a priori, no reasons why the external and/or internal sub-manifolds should be considered, separately, to be isotropic. In the context of the pre-big-bang scenario [1] the dilaton driven phase starts when the coupling constant and the curvature are quite small but this does not necessarily implies the isotropy of the expanding manifold. In fact, the study of the occurrence of a dilaton-driven, expanding, regime (in the string frame) can be connected to the problem of the gravitational collapse of a stiff (perfect) fluid in general relativity. Therefore, as it was recently shown [7], an anisotropic dilaton-driven phase can be expected also in four dimensions.

If the four-dimensional metric is *not* isotropic different phenomenological consequences can be expected both for the metric inhomogeneities and for the fluctuations of other fields (like the Kalb-Ramond axions) not contributing to the homogeneous background. Concerning the metric perturbations, it is well known that if the four-dimensional geometry

*Electronic address: m.giovannini@damtp.cam.ac.uk, giovan@cosmos2.phy.tufts.edu

¹In the present investigation we will always use the String frame, commenting, when needed, about the Einstein frame description. For a general introduction to this terminology see [1].

is completely anisotropic the scalar, vector and tensor modes of the corresponding fluctuations are all coupled [8]. More precisely the tensor modes can still be decoupled from the scalar ones, provided the four-dimensional metric possess some special symmetry [9] (like the spherical symmetry, as assumed in [7] or the cylindrical symmetry as suggested in [10]). Similar problems were addressed not in the framework of the pre-big-bang evolution but in the context of a post-big-bang (Kasner) behavior of the general relativistic solutions in the vicinity of a cosmological singularity [11,12].

In this paper we will concentrate our attention on the description of mass-less string axions fields in a fully anisotropic four-dimensional metric. Dilaton and graviton production in anisotropic string cosmological models can be studied using techniques similar to the ones we are going to exploit. There is a simple reason for this choice. In the study of the quantum mechanical inhomogeneities amplified in string cosmology the scalar and tensor modes of the metric become relevant at large frequencies [2] (i.e. small distance scales), whereas the axion and gauge perturbations seem to be more important at small frequencies where they can have interesting effects on the cosmic structures. Gauge field fluctuations can have interesting implications in the context of the problem of large scale magnetic fields [3] and in the context of large scale anisotropies [4]. Massless (Kalb-Ramond) axions interact only with couplings of gravitational strength and, therefore, their presence is not constrained by present tests of the equivalence principle. Moreover the smallness of the coupling to the anomaly makes their conversion to photons (in strong magnetic fields) negligible. Recently it was pointed out that Kalb-Ramond axions, amplified from vacuum fluctuations, can represent an interesting constraint for pre-big-bang models since they could be invoked for the generation of the CMBR anisotropy in string cosmology [5].

The purpose of our investigation is to understand which are the main consequences of treating axionic perturbations in a fully anisotropic four-dimensional metric. Our aim is to show that the evolution of the growing modes of the axionic seeds will be significantly influenced by the breaking of the isotropy with quite unexpected consequences.

Indeed in the case of four dimensional (isotropic) string cosmological metrics we have that the frequency dependence of the (logarithmic) energy spectra associated with the axion is typically “red”, i.e. the energy density of axions (in critical units) increases at large distances. This occurrence simply indicates that if we wait long enough time these fluctuations may become dominant (possibly over-closing the Universe) in the far future. If we go to the case of ten dimensional exact solutions of the low energy beta functions (of the type discussed in [1,2]) with four expanding and six contracting dimensions flat spectra of axionic fluctuations are allowed [5,6] (provided the axionic fluctuations along the internal dimensions are frozen).

The question we want to address is then the following: *if we consider the completely anisotropic case are there any indications (already in four dimension) for different spectral behaviors?* In this sense our investigation complements and extends previous studies on the subject.

In order to study this problem it is useful to review very briefly the standard results. Consider a four dimensional (isotropic) metric of pre-big-bang type [1]. Then, the Kasner-like nature of the solutions [1] implies that the curvature scale and the dilaton coupling are both growing at the same rate:

$$a(\eta) = \left[-\frac{\eta}{\eta_1} \right]^{-\frac{1}{\sqrt{3}+1}}, \quad e^{\frac{\phi}{2}} = \left[-\frac{\eta}{\eta_1} \right]^{-\frac{\sqrt{3}}{2}} \quad (1.1)$$

where ϕ is the dilaton field, and η is the conformal time coordinate. In this background the (canonically normalized) axionic fluctuation evolve according to

$$\mathcal{C}_k'' + \left[k^2 - \frac{\mathcal{G}''}{\mathcal{G}} \right] \mathcal{C}_k = 0, \quad \mathcal{C}_k = \mathcal{G} \psi_k, \quad \mathcal{G} = a e^{\frac{\phi}{2}} \quad (1.2)$$

(ψ is the axion field and the prime denotes derivation with respect to conformal time coordinate; k denotes the comoving momentum). Substituting into Eq. (1.2) the background given in Eq. (1.1) we find that the solutions of Eq. (1.2) can be expressed as linear combination of Bessel functions [15] with index $\mu = \sqrt{3}$. It can be checked that in the limit when a given mode is outside the horizon (i.e. $\eta \rightarrow 0_-$) the small argument limit of the Bessel functions leads to a growing and to a decreasing mode solutions

$$\mathcal{C}_k(\eta) \simeq c_1(k) \left[-\frac{\eta}{\eta_1} \right]^{\sqrt{3}+\frac{1}{2}} + c_2(k) \left[-\frac{\eta}{\eta_1} \right]^{-\sqrt{3}+\frac{1}{2}} \quad (1.3)$$

($c_1(k)$ and $c_2(k)$ are two integration constants fixed by the quantum mechanical normalization of the canonical mode function).

If the dilaton driven phase is followed by a radiation dominated phase it is possible to compute the logarithmic energy spectrum according to the standard techniques developed in the case of metric and gauge fluctuations [3,4] with the result that the axion energy density ρ_ψ will be given, in critical units, as

$$\Omega_\psi(\omega, \eta) = \frac{1}{\rho_c} \frac{d\rho_\psi}{d \log \omega} = g_1^2 \Omega_\gamma(\eta) \left[\frac{\omega}{\omega_1} \right]^{3-2\mu} \quad (1.4)$$

($\omega = k/a$ is the physical momentum; $\omega_1 = k_1/a \simeq (\eta_1 a)^{-1}$ is the maximal amplified frequency; $g_1 = 0.1 - 0.01$ is the value of the coupling constant at the moment of the transition from the dilaton-driven phase to the radiation dominated phase, and $\Omega_\gamma(\eta)$ is the critical fraction of energy density stored in radiation at a given time η). From Eq. (1.4) we see that if $\mu = \sqrt{3}$, as implied by the background (1.1), the spectral slope in Eq. (1.4) is $3 - 2\mu = -0.46$, namely the logarithmic energy spectrum is decreasing in frequency. Usually these type of spectra are called red simply because the largest power is stored at large distance scales. If one wants to use axionic seeds for the explanation of large scale (temperature) fluctuations in the Cosmic Microwave Background Radiation (CMBR) red spectra do not seem ideal [5] since one would need either flat or “blue” spectra (i.e. $3 - 2\mu \gtrsim 0$). As noted in [5,6] by adding six (internal) contracting dimensions and by assuming that axion fluctuations do not propagate along the internal dimensions, it is possible to achieve $\mu = 3/2$. In this case the scale factors of the external, 3-dimensional (expanding) and internal, 6-dimensional (contracting) manifolds will evolve, respectively as $a_e(\eta) \sim 9 - \eta)^{-1/4}$ and $a_i(\eta) \sim (-\eta)^{1/4}$ while the dilaton is constant [1,2]. This kind of background could also be dynamically justified not only in terms of vacuum solutions but also in terms of a string driven dynamics where the (vacuum) background equations are supplemented by (effective) string sources with negative pressure [13].

Are the conclusions of the present analysis valid in the case of a *completely anisotropic four-dimensional metric*? This is the main point we would like to investigate.

Thus, we should study which is the evolution of the (super-horizon) axion fluctuations when we drop the assumption of isotropy for the four dimensional metric. We will also have to compute precisely the spectral energy density when the axionic inhomogeneities, amplified during the anisotropic (dilaton-driven) phase, re-enter during an isotropic radiation dominated phase.

The plan of our paper is then the following. In Section II we will review the basic equations describing the dynamics of anisotropic dilaton-driven phases. We will also set up the main evolution equations of the axionic mode functions. In Section III we will study the evolution of axionic perturbations in the anisotropic models and we will show, in some analytic examples, how blue energy spectra appear. In Section IV we will concentrate our attention on numerical solutions. Finally in Section V we will study the influence of string tension corrections on our picture paying special attention to the class of models leading to blue axion (logarithmic) energy spectra. Section VI contains some final remarks and speculations.

II. BASIC EQUATIONS

The low energy string theory effective action in a four-dimensional background is

$$S = -\frac{1}{2\lambda_s^2} \int d^4x \sqrt{-g} e^{-\phi} \left[R + g^{\alpha\beta} \partial_\alpha \phi \partial_\beta \phi - \frac{1}{12} H_{\mu\nu\alpha} H^{\mu\nu\alpha} \right], \quad (2.1)$$

where $H^{\mu\nu\alpha}$ is the antisymmetric tensor field and $g_{\mu\nu}$ is a four-dimensional (spatially flat) anisotropic metric

$$g_{\mu\nu} = \text{diag}[1, -a^2(t), -b^2(t), -c^2(t)]. \quad (2.2)$$

We assume the internal compactification radii to be frozen since we want to analyse, specifically, the breaking of isotropy in the external manifold. In order to simplify our discussion we will also restrict our attention to the case where $b(t) = c(t)$. This restriction is not essential and all the results discussed in the present paper can be extended to the case of $b(t) \neq c(t)$. At the same time we find this simplification useful for the physical intuition. Notice, moreover, that if $b(t) = c(t)$ the tensor modes of the geometry propagating along the x axis can be decoupled from the scalar modes (this is not the case if $b(t) \neq c(t)$) [8,9].

The components of the antisymmetric tensor field $H^{\mu\nu\alpha}$ can be re-written in terms of a pseudo-scalar axion as

$$H^{\mu\nu\alpha} = e^\phi \frac{\epsilon^{\mu\nu\alpha\rho}}{\sqrt{-g}} \partial_\rho \psi. \quad (2.3)$$

With this choice the action (2.1) becomes

$$S = -\frac{1}{\lambda_s^2} \int d^4x \sqrt{-g} e^{-\phi} \left[R + g^{\alpha\beta} \partial_\alpha \phi \partial_\beta \phi - \frac{1}{2} e^{2\phi} g^{\alpha\beta} \partial_\alpha \psi \partial_\beta \psi \right]. \quad (2.4)$$

We want to study the situation where the axion field is not a source of the background but its fluctuations get excited by the coupled evolution of the metric and of the dilaton. By varying the action with respect to the dilaton field and with respect to the metric we obtain, after linear combinations, the tree-level evolution equations [1] for an anisotropic string cosmological model

$$\begin{aligned}\ddot{\phi}^2 - 2\ddot{\phi} + H^2 + 2F^2 &= 0 \\ \dot{\phi}^2 - H^2 - 2F^2 &= 0 \\ \dot{H} = H\dot{\phi}, \quad \dot{F} = F\dot{\phi}\end{aligned}\tag{2.5}$$

where $\dot{\phi} = \dot{\phi} - H - 2F$ and the over-dot denotes derivation with respect to the cosmic time coordinate t . The dilaton driven (vacuum) solutions of this system can be written as

$$a(t) = \left[-\frac{t}{t_1}\right]^\alpha, \quad b(t) = \left[-\frac{t}{t_1}\right]^\beta, \quad \phi(t) = (\alpha + 2\beta - 1) \log \left[-\frac{t}{t_1}\right],\tag{2.6}$$

with

$$\alpha^2 + 2\beta^2 = 1.\tag{2.7}$$

This last equation implies a Kasner-like relation for the exponents (notice that in the true Kasner case we also would have the condition $\alpha + 2\beta = 1$ which is not mandatory, in our case, in order to have a solution of the system given in Eqs. (2.5)). Notice that the solutions given in Eq. (2.5) have in general two branches connected by scale factor duality [14]. We will be mainly concerned, in our analysis, with the dilaton-driven branch where both the scale factors expand and we will comment, when required, about other (possibly relevant) phenomenological situations.

For future convenience we can express the actual solutions in conformal time coordinate (related to the cosmic time coordinate t by the usual relation $a(\eta)d\eta = dt$):

$$a(\eta) = \left[-\frac{\eta}{\eta_1}\right]^{\frac{\alpha}{1-\alpha}}, \quad b(\eta) = \left[-\frac{\eta}{\eta_1}\right]^{\frac{\beta}{1-\alpha}}, \quad \phi(\eta) = \frac{(\alpha + 2\beta - 1)}{1 - \alpha} \log \left[-\frac{\eta}{\eta_1}\right].\tag{2.8}$$

By varying the action (2.4) with respect to ψ we can obtain the evolution equation of the axionic inhomogeneities

$$\partial_\alpha \left[e^\phi \sqrt{-g} g^{\alpha\beta} \partial_\beta \psi \right] = 0\tag{2.9}$$

which can be also translated in conformal time

$$\psi'' + (\phi' + 2\mathcal{F})\psi' - \nabla_x^2 \psi - \frac{a^2}{b^2} \left[\nabla_y^2 + \nabla_z^2 \right] \psi = 0\tag{2.10}$$

where $\mathcal{F} = (\log b)'$. Defining the canonical field as $\mathcal{C} = e^{\phi/2} b \psi$ and going to Fourier space we can further modify Eq. (2.10) as

$$\mathcal{C}_k'' + \left[k_L^2 + k_T^2 \frac{a^2}{b^2} - \frac{\mathcal{G}''}{\mathcal{G}} \right] \mathcal{C}_k = 0, \quad \mathcal{G} = b e^{\frac{\phi}{2}}\tag{2.11}$$

(k_L is the modulus of the longitudinal momentum and $k_T = \sqrt{k_y^2 + k_z^2}$ is modulus of the transverse momentum). It is clear that this equation reduces to Eq. (1.2) if the background is completely isotropic. In fact taking $a \rightarrow b$ and recalling that $k = \sqrt{k_L^2 + k_T^2}$, we have that Eq. (1.2) is recovered. At the same time we can clearly see that if $a \neq b$ and the background is not isotropic Eq. (1.2) differs qualitatively from Eq. (2.11) which can also be written in a slightly different form in terms of k and of the ratio of the transverse and longitudinal momentum $r = k_T/k_L$:

$$\mathcal{C}_k'' + \left[\frac{k^2}{1 + r^2} \left(1 + r^2 \frac{a^2}{b^2} \right) - \frac{\mathcal{G}''}{\mathcal{G}} \right] \mathcal{C}_k = 0\tag{2.12}$$

In terms of the rapidity $y = (1/2) \log [(k + k_L)/(k - k_L)]$, $r = (\sinh y)^{-1}$. This form of the evolution equation will be useful in Section II for the study of the axionic (canonical) mode function \mathcal{C}_k outside the horizon. Inserting the anisotropic dilaton-driven solution of Eqs. (2.7) and (2.8) into Eq. (2.11) we obtain

$$\mathcal{C}_k'' + \left\{ k_L^2 + k_T^2 \left[-\frac{\eta}{\eta_1} \right]^\gamma - \frac{\mu^2 - \frac{1}{4}}{\eta^2} \right\} \mathcal{C}_k = 0, \quad (2.13)$$

where

$$\gamma = \frac{2(\alpha - \beta)}{1 - \alpha}, \quad 2\mu = |2\lambda - 1|, \quad \lambda = \frac{\alpha + 4\beta - 1}{2(1 - \alpha)} \quad (2.14)$$

Before dealing with the analytical and numerical solutions of Eq. (2.14) we want to present some more qualitative considerations. Comparing Eq. (1.2) to Eq. (2.13) we can notice some analogies but also crucial differences. Both equations can be seen as ‘‘Schroedinger-like’’ equations but with different ‘‘potentials’’. More specifically, one can find a similarity between Eq. (2.13) and the radial part of the Schroedinger equation in a spherically symmetric potential where the term going as η^{-2} would correspond to the (orbital) angular momentum. The term containing k_T would correspond instead to the (central) potential [15,16]. In our problem there are two relevant cases: either $\gamma < -2$ or $\gamma > -2$. If $\gamma < -2$, then the ‘‘potential’’ term might become larger, in the limit $\eta \rightarrow 0_-$ (i.e. axion fluctuations outside the horizon), than the ‘‘angular momentum’’ term. We can immediately see, amusingly enough, that this situation is never realized for the Kasner-like solutions defined by Eq. (2.7). In fact the case $\gamma < -2$ corresponds, in the (α, β) plane to $\beta > 1$ which is not realized since in the (anisotropic) vacuum solutions α and β have to lie on the ellipse $\alpha^2 + 2\beta^2 = 1$, and, therefore we will always have that $|\beta| \leq 1/\sqrt{2} \sim 0.707\dots$. Thus, we could always expect the η^{-2} term to be, at some point, dominant for $\eta \rightarrow 0_-$.

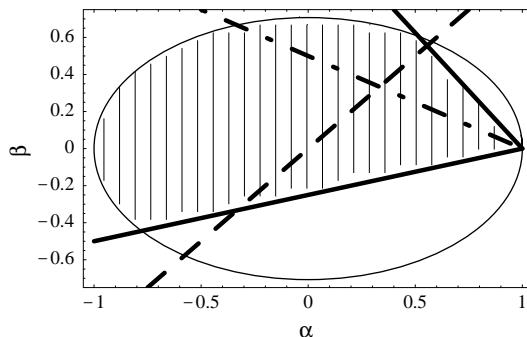


FIG. 1. We illustrate the interplay between the solutions given in Eqs. (2.6)-(2.8) and the behavior of the axionic mode function outside the horizon. The ellipse is the geometrical version of Eq. (2.7). All the α and β on the ellipse give rise to solutions of the low energy beta functions in the anisotropic metric of Eq. (2.2) with $c = b$. The arc bounded by the two full (thick) lines defines the class of anisotropic models leading to $\mu \leq 3/2$. The shading is only meant to guide the eye. The intersections of the full lines with the ellipse define the models for which $\mu = 3/2$. The dashed curve correspond to $\beta = \alpha$. For $\beta > \alpha$ (above the dashed line) we have, in Eq. (2.13) that $\gamma < 0$. The dot-dashed line corresponds to the case where $\lambda = 1/2$ (see Eq. (2.14)), implying $\mu = 0$.

In order to visualize our qualitative arguments, let us look at Fig. 1 where the ellipse is just the plot (in the (α, β) plane) of Eq. (2.7) defining the Kasner-like solution of Eqs. (2.5) and (2.8). The dashed line corresponds to $\beta = \alpha$. If $\beta > \alpha$ (above the dashed line) $\gamma < 0$ and the ‘‘potential’’ term goes to zero for $\eta \rightarrow -\infty$. Since η^{-2} becomes dominant for $\eta \rightarrow 0_-$, the solutions of Eq. (2.13) should always go to Bessel functions with index μ .

In the *anisotropic* case the index μ can be different from the Bessel index appearing in Eq. (1.2) for the *isotropic* case. Given that the (logarithmic) energy spectrum is determined by the dominant solution of Eq. (2.13) in the limit $\eta \rightarrow 0_-$, we can expect for $\mu \lesssim 3/2$ a flat or blue logarithmic energy spectrum. In the (α, β) plane the region corresponding to $\mu \lesssim 3/2$ can be obtained from Eq. (2.14) with some elementary algebra. The result is reported in Fig. 1. The arc of the ellipse bounded by the two (full) thick lines correspond to (anisotropic) vacuum solutions leading to growing modes compatible with ‘‘blue’’ spectra. The intersections between the two full lines and the ellipse correspond to the case $\mu = 3/2$ (flat spectrum). Of course not all the models within the full lines are realistic.

For examples we could have, in principle, growing spectra with $\alpha > 0$ and $\beta > 0$ (first quadrant). These models are clearly *not* realistic since they would describe a dilaton-driven contraction more than a dilaton-driven expansion. More realistic are the models in the second quadrant where one of the two scale factors expands and the other contracts.

Finally in the third quadrant we have the most physical situation where the two scale factors *both expand*, though at different rates. It is amusing to notice that the intersection between the full line and the ellipse picks up a dilaton-driven solution with $\mu = 3/2$ and expanding scale factors. The lower full line has equation $4\beta = (\alpha - 1)$ and the intersection we are interested occurs for $\alpha = -7/9$ and $\beta = -4/9$. Going to Eq. (2.8) we see that, in this case

$\phi(\eta) \sim -3/2 \log[-\eta/\eta_1]$. In this case, on the basis of the asymptotic behavior of Eq. (2.13) in the small $|\eta|$ limit, the solution outside of the horizon will be given by

$$\mathcal{C}_k(\eta) \simeq c_1(k) \left[-\frac{\eta}{\eta_1}\right]^{-1} + c_2(k) \left[-\frac{\eta}{\eta_1}\right]^2. \quad (2.15)$$

which coincides with the solution one would obtain in the ten-dimensional case where the external manifold has scale factor $a_e(\eta) \sim (-\eta)^{-1/4}$ and the internal one has scale factor $a_i \sim (-\eta)^{1/4}$.

Another interesting case is represented by the model $\alpha = -1$ and $\beta = 0$. In this case $\phi(\eta) \sim -\log[-\eta/\eta_1]$. This solution might not seem fully realistic and indeed we will use it as a toy model. At the same time one can argue that this type of solutions might be the result, in the pre-big-bang scenario, of spherically symmetric initial conditions which are asymptotically trivial in the past [7]. It is quite amusing to work out the Einstein frame description of this solution. The Einstein frame scale factors are related to the ones of the String frame by trivial conformal rescalings involving the dilaton, namely

$$\tilde{a} = e^{-\frac{\phi}{2}} a, \quad \tilde{b} = e^{-\frac{\phi}{2}} b. \quad (2.16)$$

Since the conformal time coordinate does not change passing from one frame to the other (i.e. $d\eta \equiv d\tilde{\eta}$ we can obtain easily that, in the Einstein frame, our solution looks like $\tilde{a} \sim \text{const.}$ and $\tilde{b} \sim \sqrt{-t}$ (since $\tilde{a}(\eta)$ is constant t and η coincide up to a constant factor).

It is interesting to point out that this solution was Kasner-like in the String frame (i.e. $\alpha^2 + 2\beta^2 = 1$) and it becomes true Kasner in the Einstein frame. This solution is well known in the theory of the gravitational collapse [17] and it might be thought as the limit (in the vicinity of the singularity) of a spherically symmetric space filled with a stiff (perfect) fluid. It was indeed recently stressed that the Einstein frame description dilaton-driven cosmologies in four dimensions is closely connected with the problem of the gravitational collapse of a stiff fluid and that, consequently, string cosmological models of pre-big-bang type are as fine-tuned as the gravitational collapse [7].

If $\alpha = -1$ and $\beta = 0$ we have that in Eq. (2.13) $\gamma = -1$. It is amusing to notice that in this case the Eq. (2.13) is analytically solvable and it is (formally) equivalent to the Schroedinger equation in a Coulomb potential with complex electromagnetic coupling. We will use this analogy in the next section. For the moment we can guess that outside the horizon the solution to Eq. (2.13) will be well approximated by

$$\mathcal{C}_k = c_1(k) \left[-\frac{\eta}{\eta_1}\right]^{\frac{3}{2}} + c_2(k) \left[-\frac{\eta}{\eta_1}\right]^{-\frac{1}{2}}. \quad (2.17)$$

Again this solution was simply obtained by solving Eq. (2.13) in the small η limit where the ‘‘Coulomb’’ contribution can be neglected. Since this is nothing but the small argument limit of Hankel functions with $\mu = 1$, we again argue that the exact solution should give us a blue (logarithmic) energy spectrum of the type of the one given in Eq. (1.2) with spectral index $3 - 2\mu = 1$.

III. BLUE SPECTRA

In some cases, analytical solutions of Eq. (2.13) can be found. We start to discuss blue spectra and, more precisely we analyze the model mentioned in the previous Section with $\alpha = -1$. In this case Eq. (2.13) becomes, using k and r

$$\mathcal{C}_k'' + \left\{ \frac{k^2}{1+r^2} \left[1 + r^2 \left(-\frac{\eta}{\eta_1} \right)^{-1} \right] - \frac{3}{4\eta^2} \right\} \mathcal{C}_k = 0. \quad (3.1)$$

This equation looks indeed very similar to the (radial) Schroedinger equation for the Coulomb problem. In order to solve Eq. (3.1) we have to match the standard notations appearing in the theory of special functions [15]. Defining a new (complex) time as

$$\tau = \frac{2ik\eta}{\sqrt{1+r^2}} \quad (3.2)$$

we can re-write Eq. (3.1) as

$$\frac{d^2 \mathcal{C}_k}{d\tau^2} + \left[-\frac{1}{4} + \frac{\zeta}{\tau} - \frac{3}{4\tau^2} \right] \mathcal{C}_k = 0 \quad (3.3)$$

with $\zeta = (i/2)\epsilon r$. It is helpful to define $\epsilon = k_T \eta_1 = k \eta_1 r / \sqrt{1+r^2}$ purely for algebraic reasons. Eq. (3.3) is one of the well known forms of the Whittaker's equation [15] whose solutions are the corresponding Whittaker's functions, related to confluent hypergeometric functions. We are interested in solutions which represent incoming axionic waves for $\eta \rightarrow -\infty$ and then our solution will have the form

$$W_k(\tau) = e^{-\frac{\pi}{2}\tau^{\frac{3}{2}}} U\left[\frac{3}{2} - \frac{i}{2}\epsilon r, 3, \tau\right] \quad (3.4)$$

where $U[m, n, \tau]$ is the (Kummer) confluent hypergeometric function with parameters m and n . Therefore the (properly normalized) form of the solution of Eq. (3.1) is

$$C_k(\eta) = \frac{1}{\sqrt{k}} \sqrt{\frac{2}{\pi}} e^{-i\frac{k\eta}{\sqrt{1+r^2}} + i\frac{\pi}{4}} \left[\frac{2ik\eta}{\sqrt{1+r^2}} \right]^{\frac{3}{2}} U\left[\frac{3}{2} - \frac{i}{2}r\epsilon, 3, 2i\frac{k\eta}{\sqrt{r^2+1}}\right]. \quad (3.5)$$

We can immediately notice, as expected, that the small argument limit of the previous solution (i.e. $k\eta \ll 1$) exactly reproduces the asymptotic evolution obtained in Eq. (2.17).

Having derived the solution of Eq. (3.1) we can also compute the energy spectrum of the axions amplified by the transition from an anisotropic dilaton-driven solution to a (completely isotropic) radiation dominated epoch occurring at $\eta = -\eta_1$. For $\eta > -\eta_1$ the evolution equation of the axion fluctuations will be given by

$$C_k'' + k^2 C_k = 0, \quad (3.6)$$

because the dilaton coupling freezes, after $-\eta_1$, to a constant value. A similar calculation was performed in [5] under the assumption that the isotropisation of the geometry occurred prior to the onset of the dilaton-driven phase (indeed described, in [5] only by one scale factor).

The frequency mixing coefficient $c_-(k)$, determining the spectral number of produced axions, can be explicitly computed by matching, at $\eta = -\eta_1$ the general ‘‘outgoing’’ solution of Eq. (3.6)

$$C_k(\eta) = \frac{1}{\sqrt{k}} \left[c_+ e^{-ik(\eta+\eta_1)} + c_- e^{ik(\eta+\eta_1)} \right], \quad \eta > -\eta_1, \quad (3.7)$$

to the ‘‘incoming’’ solution (3.5) of Eq. (3.1) which represents positive frequency modes in the $\eta \rightarrow -\infty$ limit (notice, however, that the incoming solution does not define, asymptotically a Bunch-Davies vacuum because of the presence of the term ‘‘Coulomb’’ term in Eq. (3.1) which is dominant in the far past).

Following this procedure we determined the mixing coefficients reported in Appendix A. The important point to mention is that for $k\eta_1 > 1$ the procedure leading to the mixing coefficients is no longer valid but the mixing coefficient can be anyway estimated by using in Eq. (3.1) a smooth ‘‘potential’’ interpolating between $\eta < -\eta_1$ and $\eta > -\eta_1$. For $k\eta_1 > 1$ the mixing coefficients are indeed exponentially suppressed [18] and can be ignored for the purpose of this paper. Therefore, taking the limit (for $k\eta_1 < 1$) of the results reported in Appendix A we have

$$|c_-(x_1)| \simeq \frac{[S(r)]^{-1/2}}{4\pi} x_1^{-3/2} \quad (3.8)$$

where $S(r) = 1/\sqrt{r^2+1}$ and $x_1 = k\eta_1$.

The spectral energy density

$$\rho_\omega = \frac{d\rho_\psi}{d\log\omega} \simeq \frac{\omega^4}{\pi^2} |c_-(\omega)|^2 \quad (3.9)$$

is the variable frequently adopted to characterize the distribution of the produced particles [2,3,5], for our case reads

$$\Omega_\psi(\omega, \eta) = \frac{\rho_\omega}{\rho_c} = \frac{g_1^2 \Omega_\gamma(\eta)}{16\pi^4 S(r)} \left(\frac{\omega}{\omega_1} \right) \quad (3.10)$$

where ρ_c is the critical energy density and $\Omega_\psi(\omega, \eta)$ is the (critical) fraction of produced (mass-less) Kalb-Ramond axions. Notice that $n(\omega) = |c_-(\omega)|^2$ can be interpreted, in a fully quantum mechanical treatment of the processes of cosmological particle production [2,19], as the mean number of axions with physical momentum ω . In Eq. (3.10) $g_1 = e^{\phi(\eta_1)/2} \sim 0.1 - 0.01$ is the final value of the string coupling parameter at the time of the transition to the radiation dominated epoch. In terms of g_1 the string and Planck mass are related as $M_s = g_1 M_P$.

The spectral slope appearing in Eq. (3.10) is exactly the one we guessed in Section II using the approximate solution of Eq. (2.13) in the small η limit for the axion mode function. The result is that the spectral energy density is only slightly tilted towards large frequencies. We remind, incidentally, that in string cosmological models blue spectra are also possible for gauge fields [4], but not for metric fluctuations [2]. In the case of gravitons, for example, the typical slope for the spectral energy density is close to 3 (“violet” energy spectra).

Thus also in the fully anisotropic case the spectral distribution of the amplified axions is determined by the solution of the mode equation in the small η limit. Furthermore, on the basis of the analytical treatment performed in the present Section we can argue that as long as $\gamma > -2$ in Eq. (2.13), the spectral slope of the spectral energy density ρ_ω is completely determined by the “angular momentum” term appearing in Eq. (2.13). On the other hand the spectral amplitude does depend upon the details of the particular anisotropic model and upon the relative weight of the longitudinal and transverse momentum (i.e. $r = k_T/k_L$) during the anisotropic phase. In particular if $r \rightarrow 0$ (i.e. $k_T \ll k_L$) $S(r) \rightarrow 1$. In the large r limit (i.e. $k_T \gg k_L$) $S(r) \sim r$. From a physical point of view, $r \sim 1$ implies a fairly isotropic (initial) momentum distribution and it makes sense only when $a(\eta) \rightarrow b(\eta)$. Conversely, r very different from 1 implies either the dominance of transverse momenta or the dominance of the longitudinal momenta. We see that r cannot be arbitrarily large since we have always to demand $\Omega(\omega, \eta) < 1$. Imposing the critical energy bound on the axion fluctuations we get, indeed, that $r < 16\pi^4/g_1^2$ (i.e. $r < 10^5$ if $g_1 = 0.1$).

One can understand, more physically, the r and $k\eta_1$ dependence by looking more closely at Eq. (3.1). Let us write the “Coulomb” potential and the “angular momentum” in a rescaled form, namely

$$f(\xi, x_1, r) = \frac{x_1^2 r^2}{r^2 + 1} \frac{1}{\xi} - \frac{3}{4\xi^2} \quad (3.11)$$

where $\xi = [-\eta/\eta_1]$ and, as usual, $x_1 = k\eta_1$. The plot of the function (3.11) for (different values of the parameters) is reported in Fig. 2.

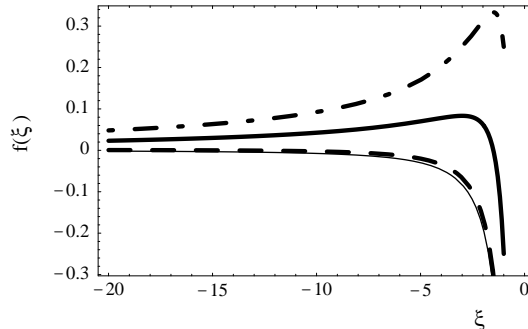


FIG. 2. We plot different regimes of Eq. (3.11). With the thick (full) line we have the case $x_1 = 1$ and $r = 1$. With the dashed line we illustrate the case $x_1 = 0.1$, $r = 1$, whereas with the dot-dashed line we illustrate the case $x_1 = 1$ and $r = 10^3$. Notice that the thin (full) line is for the case $x_1 = 0.001$, $r = 1$.

Since we want to consider modes which are amplified (and not exponentially suppressed) we have to focus on the case $x_1 \lesssim 1$. From Fig. 2 we learn that as soon as x_1 gets smaller and smaller (i.e. frequencies smaller than the maximal) the “Coulomb” term in Eq. (3.11) gets even more negligible if compared with the term going as ξ^{-2} . Moreover, for large r and high frequencies (i.e. $x_1 \sim 1$) the potential barrier gets higher. Thus, if we are going to explore a frequency range $k \ll \eta_1^{-1}$ (i.e. $\omega \ll \omega_1$) our approximation improves.

IV. FLAT SPECTRA

Having discussed the case of a specific blue spectrum we want now to treat the case of a flat spectrum in anisotropic dilaton-driven models. We argued in Section II that in order to obtain a flat spectrum we have to require $\mu = 3/2$, which does correspond either to $\alpha = 1$ and $\beta = 0$ or to $\alpha = -7/9$ and $\beta = -4/9$. The case $\alpha = 1$ $\beta = 0$ is clearly *not realistic*: it does correspond to a contracting Universe (in the string frame). The interesting case is indeed the second where the dilaton growth triggers a superinflationary phase where the different dimensions expand with different rates:

$$a(t) \sim \left[-\frac{t}{t_1} \right]^{-\frac{7}{9}}, \quad b(t) \sim \left[-\frac{t}{t_1} \right]^{-\frac{4}{9}}, \quad \phi(t) = -\frac{8}{3} \log \left[-\frac{t}{t_1} \right]. \quad (4.1)$$

For this background the explicit form of Eq. (2.13) is

$$\mathcal{C}'' + \left\{ \frac{k^2}{1+r^2} \left[1 + r^2 \left(-\frac{\eta}{\eta_1} \right)^{-3/8} \right] - \frac{2}{\eta^2} \right\} \mathcal{C} = 0, \quad (4.2)$$

which becomes, going to dimensionless (conformal) time,

$$\frac{d^2 \mathcal{C}}{d\xi^2} + \left\{ \frac{x_1^2}{r^2 + 1} - h(\xi, x_1, r) \right\} \mathcal{C} = 0, \quad \xi = \frac{\eta}{\eta_1}, \quad (4.3)$$

where

$$h(\xi, x_1, r) = \frac{r^2}{r^2 + 1} \frac{x_1^2}{\xi^{3/8}} - \frac{2}{\xi^2}. \quad (4.4)$$

In Eq. (4.4) the analogous of the Coulomb term goes as $\xi^{-3/8}$. Therefore, we expect the (numerical) solutions of Eq. (4.3) to converge more slowly than in the case of Eq. (2.17) to the solution one would guess taking into account only the leading contribution for small ξ . This is illustrated in Fig. 3 where the function $h(\xi)$ is reported for different values of the parameters.

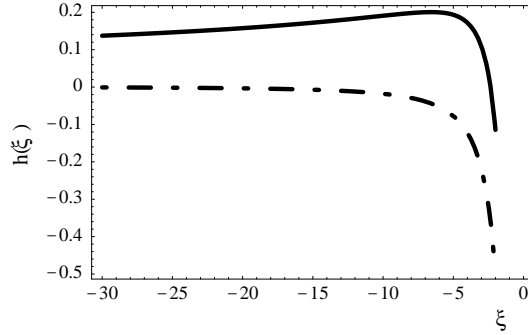


FIG. 3. We illustrate different cases of Eq. (4.4). With the thick (full) line we have the case $x_1 = 1$ and $r = 1$. With the dashed line we plot the case $x_1 = 0.1$, $r = 10$.

Eq. (4.3) can be solved numerically. In Fig. (4) the numerical solutions of Eq. (4.3) are reported for different values of the primordial rapidity. For comparison (dashed lines) we also report, for the same values of the parameters, the behavior of the approximate solutions of Eq. (4.3) obtained by neglecting the term $\xi^{-3/8}$. For $x_1 \lesssim 0.001$ the approximate solutions can be definitely trusted in the small ξ limit.

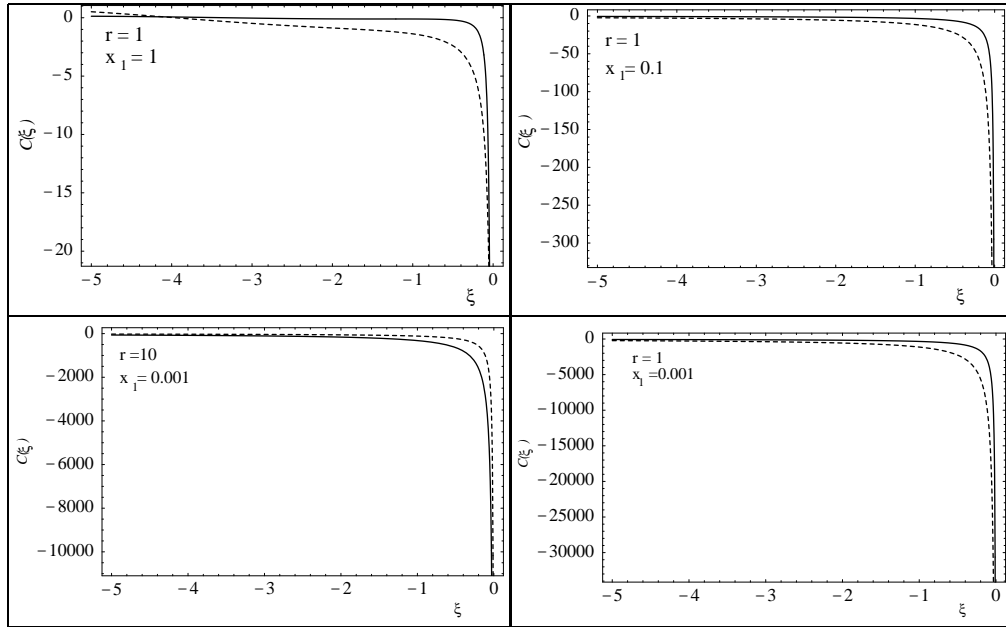


FIG. 4. We report the numerical solutions of Eq. (4.3) for decreasing values of x_1 . We also report the approximate solutions (dashed curves) given in Eq. (4.5).

The approximate solutions plotted with the dashed line in Fig. (4) are

$$\mathcal{C}(\xi) = \frac{1}{\sqrt{k}} \sqrt{\xi x_1 S(r)} \{ J_{3/2}[\xi x_1 S(r)] - i Y_{3/2}[\xi x_1 S(r)] \} \quad (4.5)$$

By directly matching Eq. (4.5) with Eq. (3.7) we obtain that the relevant mixing coefficient is

$$|c_-|^2 \sim \mathcal{K}(r) \frac{1}{8\pi^2 S(r) x_1^4} \quad (4.6)$$

corresponding to

$$\Omega_\psi(\omega, \eta) = \frac{\rho_\omega}{\rho_c} = \frac{\mathcal{K}(r)}{16\pi^4 S(r)} g_1^2 \Omega_\gamma(\eta) \quad (4.7)$$

Notice that $\mathcal{K}(r)$ is a (frequency independent) factor which can be precisely determined numerically and which becomes important in the limit $x_1 \sim 1$. If $x_1 \lesssim 0.001$, $\mathcal{K}(r) \sim 1$.

It would be desirable to find approximate (but analytical) expressions describing the evolution of the mode function outside of the horizon in the general case of anisotropic backgrounds of the type of the one introduced in Eq. (2.8). The evolution equation (2.11) for the axionic mode function can be written as

$$\mathcal{C}_k'' + \left[k^2 - V_k(\eta) \right] \mathcal{C}_k = 0, \quad V_k(\eta) = \frac{k^2 r^2}{1+r^2} \left(\frac{b^2 - a^2}{b^2} \right) + \frac{\mathcal{G}''}{\mathcal{G}} \quad (4.8)$$

The effective potential appearing in Eq. (4.8) generalizes the previous results of Eqs. (3.11) and (4.4). Notice that the situation of a k -dependent effective potential is not so uncommon since it arises in the case of perturbations of kaluza-Klein backgrounds with fluctuating internal dimensions [2] and in the case gravitational waves propagating in a background whose action contains higher derivatives [21]. Notice also that in the isotropic limit (i.e. $b \rightarrow a$) Eq. (4.8) goes to Eq. (1.2) since $\mathcal{G} \rightarrow ae^{\phi/2}$ and the term proportional to the anisotropy (i.e. $(b^2 - a^2)/b^2$) exactly vanishes. We want to solve Eq. (4.8) in the limit $\eta \rightarrow 0_-$ and show that the correction to the leading order solution (obtained by dropping the $b^2 - a^2/b^2$ term) is indeed small. The equation we have to solve is essentially

$$C_k'' \simeq V_k(\eta) C_k. \quad (4.9)$$

By writing the solution to Eq. (4.9) as

$$C_k(\eta) \sim \bar{C}_k(\eta) + \epsilon_k(\eta), \quad (4.10)$$

where \bar{C}_k is the leading order solution

$$\bar{C}_k \sim A \mathcal{G}(\eta) + B \mathcal{G}(\eta) \int^\eta \frac{d\eta'}{\mathcal{G}(\eta')^2} \quad (4.11)$$

we can find that $\epsilon_k(\eta)$ is simply given by

$$\epsilon_k(\eta) \sim \frac{k^2 r^2}{1+r^2} \mathcal{G}(\eta) \int^\eta \mathcal{G}(\tau) \bar{C}_k(\tau) \left(\frac{b^2 - a^2}{b^2} \right) \int^\tau \frac{d\eta''}{\mathcal{G}(\eta'')^2} \quad (4.12)$$

(A and B are arbitrary constants). Notice, again, that the correction vanishes exactly for $b \rightarrow a$. If we insert in the previous equations the background solutions of Eq. (2.8) we get

$$\begin{aligned} C_k(\eta) \sim & A \left\{ \left(-\frac{\eta}{\eta_1} \right)^\lambda + \frac{(k\eta_1)^2}{2(\gamma+1)(1-2\lambda)} \frac{r^2}{1+r^2} \left[(\gamma+1) \left(-\frac{\eta}{\eta_1} \right)^{\lambda+2} - 2 \left(-\frac{\eta}{\eta_1} \right)^{\gamma+1+2\lambda} \right] \right\} \\ & + B \left\{ \frac{1}{1-2\lambda} \left(-\frac{\eta}{\eta_1} \right)^{1-2\lambda} + \frac{(k\eta_1)^2}{(1-2\lambda)^2(3-2\lambda)(3-\lambda+\gamma)} \frac{r^2}{r^2+1} \left[(3-2\lambda+\gamma) \left(-\frac{\eta}{\eta_1} \right)^{3-\lambda} \right. \right. \\ & \left. \left. - (3-2\lambda) \left(-\frac{\eta}{\eta_1} \right)^{3-\lambda+\gamma} \right] \right\} \end{aligned} \quad (4.13)$$

In each of the curly brackets the first term is the leading solution whereas the term proportional to $(k\eta_1)^2$ is the correction. Notice that the correction is subleading in the limit $\eta \rightarrow 0_-$. Take, for instance, the case investigated in this section, namely $\lambda = -1$ and $\gamma = -3/8$. We can easily find, from Eq. (4.13)

$$\begin{aligned}
\mathcal{C}_k(\eta) \sim & A \left\{ \left(-\frac{\eta}{\eta_1} \right)^{-1} + \frac{4}{39} (k\eta_1)^2 \frac{r^2}{r^2+1} \left[\frac{13}{8} \left(-\frac{\eta}{\eta_1} \right) - 2 \left(-\frac{\eta}{\eta_1} \right)^{\frac{5}{8}} \right] \right\} \\
& + B \left\{ \frac{1}{3} \left(-\frac{\eta}{\eta_1} \right)^2 + \frac{(k\eta_1)^2}{370} \frac{r^2}{r^2+1} \left[\frac{37}{8} \left(-\frac{\eta}{\eta_1} \right)^4 - 5 \left(-\frac{\eta}{\eta_1} \right)^{\frac{29}{8}} \right] \right\}
\end{aligned} \tag{4.14}$$

Notice that the leading super-horizon contribution to the evolution of the axionic mode function is given, as expected, by the term going as η^{-1} appearing in the first curly bracket. In both the curly bracket we have the term $(k\eta_1)^2$ which is always smaller than one since η_1^{-1} is the maximal amplified frequency. Moreover, in both the curly brackets all the terms multiplied by $(k\eta_1)^2$ are vanishingly small outside the horizon. We could repeat the same calculation by inserting different (expanding) anisotropic backgrounds into Eq. (4.13). We find that for the class of models defined on the arc of the “vacuum” ellipse depicted in Fig. 1 all the corrections are indeed small and the leading contribution is given, as foreseen, by the growing mode. Notice that we already knew that from the considerations of Section I and II. In the present approach we are also able to compute, analytically, the corrections to the leading solution.

V. ANISOTROPY AND STRING TENSION CORRECTION

The main assumption behind the calculations we presented has been the presence of an *anisotropic* string cosmological phase. In previous calculations [5,6] the axion spectra were actually computed assuming that the (four dimensional) background describing the dilaton-driven dynamics was completely *isotropic*. Therefore, in [5,6] it was also implicitly assumed that the isotropization of the four (expanding) dimensions occurred prior to the onset of the dilaton-driven evolution. As we stressed in Section II, to assume that the dilaton driven phase was *not* completely isotropic might be natural from the point of view of the “asymptotic past triviality” of the pre-big-bang scenario [7]. More specifically, the comparative study of (spherically symmetric) gravitational collapse and pre-big-bang scenario seem to imply the occurrence of anisotropic dilaton driven phases. As we stressed, the example given in Section III can be interpreted, from the point of view of the background evolution in the Einstein frame, as the gravitational collapse of a sphere filled with a perfect (stiff) fluid [17] leading, ultimately, to an anisotropic four-dimensional dilaton-driven phase in the string frame picture.

The fact that anisotropic initial conditions are generally allowed by the solutions of the tree-level action might not be, in principle, sufficient in order to justify our assumptions. In fact what we need for our considerations is a metric which is anisotropic not only locally (i.e. for a short amount of time in the dilaton-driven phase) but globally (i.e. for all the duration of the dilaton-driven phase). What might happen is that the addition of higher string tension corrections to the tree-level action forbid the presence of a (long) anisotropic phase. If the anisotropic phase is not sufficiently long the axion fluctuations will not have enough time to fully develop their growing modes.

A fair measure of the anisotropy of a four-dimensional metric can be given, in our particular case as

$$A(t) \equiv \frac{H - F}{\dot{V}} = \frac{3(H - F)}{H + 2F}, \quad V(t) = \frac{\log[\sqrt{-g}]}{3}, \tag{5.1}$$

(this type of measure for the anisotropy of a four-dimensional geometry was introduced long ago by Zeldovich [20]). Notice that, in the isotropic limit (i.e. $H \rightarrow F$), $\dot{V}(t)$ coincides with the Hubble factor and $A(t) \rightarrow 0$. Another possible measure of the degree of anisotropy of a (homogeneous) background geometry can be also given as the ratio between the Weyl and Riemann invariants

$$B(t) = \frac{C_{\mu\nu\alpha\beta} C^{\mu\nu\alpha\beta}}{R_{\mu\nu\alpha\beta} R^{\mu\nu\alpha\beta}}, \tag{5.2}$$

which is supposed to vanish in the isotropic limit (see Appendix B for the explicit expression of $B(t)$ in our background geometry).

Consider now a dilaton driven-phase evolving according to the solutions discussed in the previous section, i.e. $H \sim -7/(9t)$ and $F \sim -4/(9t)$. Then $A(t) \sim 3/5$. The question is then the following: if we introduce quadratic corrections to the tree-level action will $A(t)$ be roughly constant for the whole duration of the dilaton driven phase? In other words: can we show that A is roughly frozen to the value given by the dilaton-driven “vacuum” solutions prior to the onset of the stringy phase where the curvature is stabilized? If this is not the case, namely if $A(t)$ is not constant during the dilaton-driven phase, then the anisotropy in the background will only be local.

Let us start from the string effective action supplemented by the first string tension correction in four (anisotropic) dimensions. We follow the notation of [22] where this problem was studied in the string frame picture (see also [23] for the discussion of similar problems in the Einstein frame picture):

$$S = -\frac{1}{2\lambda_s^2} \int d^4x \sqrt{-g} e^{-\phi} \left[R + g^{\alpha\beta} \partial_\alpha \phi \partial_\beta \phi - \frac{w\lambda_s^2}{4} \left(R_{GB}^2 - (g^{\alpha\beta} \partial_\alpha \phi \partial_\beta \phi)^2 \right) \right], \quad (5.3)$$

where R_{GB}^2 is simply the Gauss-Bonnet invariant expressed in terms of the Riemann, Ricci and scalar curvature invariants

$$R_{GB}^2 = R_{\mu\nu\alpha\beta} R^{\mu\nu\alpha\beta} - 4R_{\mu\nu} R^{\mu\nu} + R^2, \quad (5.4)$$

and w is a numerical constant of order 1 which can be precisely computed depending upon the specific theory we deal with (for instance $w = -1/8$ for heterotic strings). Notice that in [19] this problem was discussed in greater generality. Here we will recall and extend the topics which are directly relevant in our investigation.

It is convenient, for the problem at hand, not to synchronize immediately the clocks. Therefore the metric will be

$$g_{\mu\nu} = \text{diag}[N(t)^2, -a(t)^2, -b(t)^2, -b(t)^2]. \quad (5.5)$$

Notice that by fixing the lapse function to 1 corresponds to the synchronous coordinate frame. Inserting Eq. (5.5) into Eq. (5.3) we get, after integrating by parts the derivatives of the lapse function,

$$S = \frac{1}{2\lambda_s^2} \int dt e^{\alpha+2\beta-\phi} \left\{ \frac{1}{N} \left[-\dot{\phi}^2 - 2\dot{\beta}^2 - 4\dot{\alpha}\dot{\beta} + 2\dot{\alpha}\dot{\phi} + 4\dot{\beta}\dot{\phi} \right] + \frac{w\lambda_s^2}{4N^3} \left[8\dot{\phi} \dot{\alpha} \dot{\beta}^2 - \dot{\phi}^4 \right] \right\} \quad (5.6)$$

where we used the notation $a(t) = e^{\alpha(t)}$, $b(t) = e^{\beta(t)}$. We can take the variation of this action with respect to N , α , β and ϕ and we will get three dynamical equations supplemented by a constraint connecting the first derivatives of the fields. These equations are reported in Appendix B. Here we give the final expression of the system of nonlinear differential equations obeyed by $x \equiv \dot{\alpha}$, $y \equiv \dot{\beta}$, $z \equiv \dot{\phi}$:

$$\dot{x} = \left\{ \frac{-[-8y^2 + 8yz - 4z^2 + z^4 + 8x^2(-1 + yz) + 8x(z + y^2z - y(1 + z^2))]}{8(-1 + yz)} \right\} + \left[\frac{1 - xz}{-1 + yz} \right] \dot{y} + \left[\frac{-1 - xy}{-1 + yz} \right] \dot{z} \quad (5.7)$$

$$\dot{y} = \left[\frac{-8(3y^2 + x^2(1 + y^2) + 2x(y + y^3)) + 8(x + 2y)z - 4z^2 + 4(x + 2y)z^3 - 3z^4}{16(1 + xy)} \right] + \left[\frac{2 + 3z^2}{4 + 4xy} \right] \dot{z} + \left[\frac{-(1 + y^2)}{2(1 + xy)} \right] \dot{x} \quad (5.8)$$

$$\dot{z} = \left\{ \frac{-[16yz + 16y^3z + z^2(-4 + z^2) - 8y^2(3 + z^2)]}{8(1 + y^2)} \right\} + \left[\frac{2(1 - yz)}{1 + y^2} \right] \dot{y} \quad (5.9)$$

It is known from previous studies [19] that this system of nonlinear differential equations admits an isotropic fixed point which can be obtained by setting $x = y = \text{constant}$ in the constraint given in Eq. (B.1) which will give a consistency condition which leading to $x = y = 0.616\dots$ and $z = 1.414\dots$. It is also known that this (isotropic) fixed point can attract (mildly) anisotropic dilaton-driven cosmologies [19]. The question we have to address, in our context, is threefold. First of all we have to ask if the anisotropic models we are interested in from the previous sections are attracted towards this isotropic fixed point. If this is the case we have to investigate how the anisotropic phase is analytically connected with the isotropic phase with constant (and regular) curvature. Finally we have to understand quantitatively how long is the duration of the anisotropic phase before the isotropization (triggered by the string tension corrections) takes place.

In our present notation we have, from Eq. (5.1) that

$$A(t) = \frac{3[x(t) - y(t)]}{x(t) + 2y(t)}. \quad (5.10)$$

In order to answer the previous questions we will integrate numerically the system given in Eqs. (5.7)–(5.9) imposing, at the initial integration time, $A(t_0) = 3/5$ which is equivalent to impose initial conditions will along the lines $\dot{\phi} = (9/7)H$ and $\dot{\phi} = (9/4)F$ in the $(\dot{\phi}, H)$ and $(\dot{\phi}, F)$ planes. Our results are reported in Fig 5. We see, in this particular case, that the model, initially anisotropic, is indeed attracted towards its isotropic fixed point by virtue of the string tension corrections.

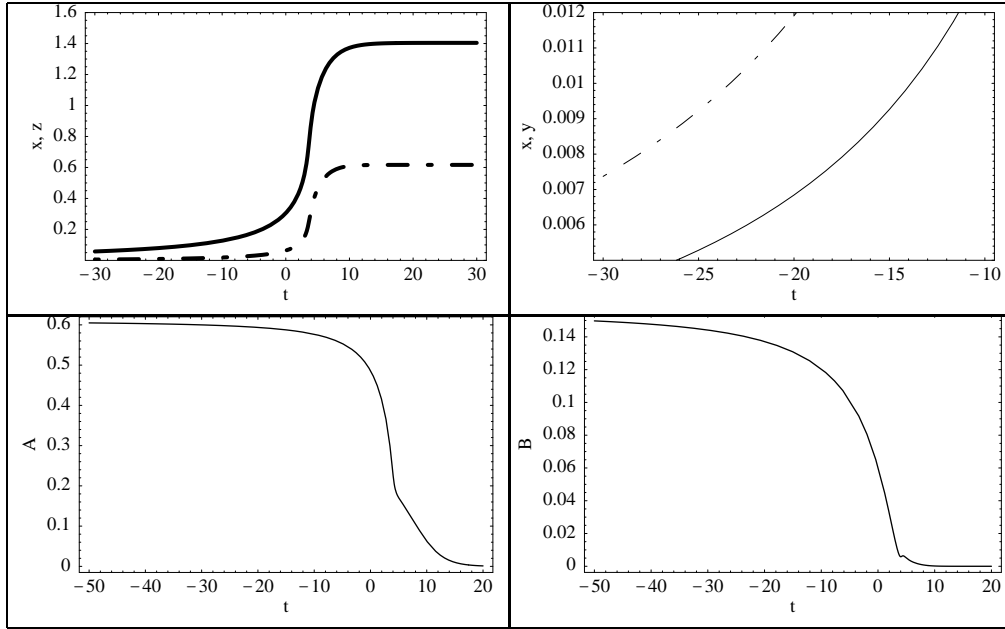


FIG. 5. In the two upper plots we report the behavior of x , y and z . At the top left the evolution of z (thick full line) is compared with the evolution of x (dot-dashed thick line). We see that they both freeze to a constant value given by the isotropic fixed point. Also y reaches, for large t its isotropic limit but, during the dilaton-driven phase the background is anisotropic. In the top right plot we show indeed the evolution of x (thin dot-dashed line) and y (thin full line) prior to the isotropization occurring at the onset of the stringy phase. This point is also stressed in the two lower plots. In the bottom left plot we report the numerical evaluation of the asymmetry given in Eq. (5.1). We can see that it goes to zero for large positive times but it is roughly constant during the dilaton-driven phase. In the bottom right plot we illustrate the same qualitative evolution of the ratio between the Weyl and the Riemann invariants reported in Eqs. (5.2) and (B.7).

The curvature invariants (including the Weyl invariant) are all regular. Moreover the Weyl invariant and the asymmetry defined in Eq. (5.1) both vanish for large times signaling that the isotropy is indeed recovered. The anisotropic and the isotropic phase are then connected and the anisotropic regime lasts as long as $B(t)$ and $A(t)$ are almost frozen to their constant values (fixed by the initial conditions). This evolution is typical, in our examples, for negative times. In this regime the solutions are the ones discussed in Section II and, therefore the typical behavior of the axionic growing modes is different from the one dictated by a completely isotropic dilaton driven dynamics and leading to red logarithmic energy spectra. By solving Eqs. (5.7)–(5.9) together with Eq. (2.10), we checked that, as far as the dilaton driven phase is concerned, the axionic growing modes are indeed the ones we computed by using the tree-level solutions discussed in Section II. We will report this study elsewhere.

One can ask, at this point, how general is this behavior. Our answer is that it holds for various models which we would call mildly anisotropic, from the point of view of their initial (primordial) asymmetry. The results we just presented in a particular case do not hold in the case of strongly anisotropic initial conditions where, for example, one of the two scale factors contracts (in the string frame) instead of expanding like the ones appearing in the second quadrant of the plot reported in Fig. 1, like, for instance the case where $\alpha = -1/3$ and $\beta = 2/3$. Since for the (anisotropic) dilaton-driven solutions discussed in Section II we have that the asymmetry is

$$A(t_0) = 3 \frac{(\alpha - \beta)}{\alpha + 2\beta} \quad (5.11)$$

we have for $\alpha = -1/3$ and $\beta = 2/3$ that $A(t_0) = -3$. With these initial conditions the system of Eqs. (5.7)–(5.9) evolves towards a singularity, the isotropic fixed point is not reached and the anisotropic phase lasts forever. Moreover, we can see that the asymmetry grows (in modulus) becoming more and more negative. In this case the string tension corrections will make the geometry more and more anisotropic.

Therefore we studied the accelerated branch of the dilaton driven solutions (i.e. $\alpha < 0$ and $\beta < 0$) and we fixed the initial conditions of the system (5.7)–(5.9) by requiring that

$$A(t_0) = 3 \frac{(-\sqrt{1 - 2\beta^2} - \beta)}{-\sqrt{1 - 2\beta^2} + 2\beta} \quad (5.12)$$

(where we simply inserted $\alpha = -\sqrt{1 - 2\beta^2}$ into Eq. (5.11) in order to force the initial conditions to lie inside the space of the solutions of the tree level action [see also Fig. 1]). We then moved β in the range $-0.333(3) \lesssim \beta < 0$ where, according to Fig. 1, blue axionic spectra are expected on the basis of the tree-level dilaton driven solutions. Our results are reported in Fig. 6 in terms of the two previously introduced estimators of the anisotropy $A(t)$ and $B(t)$. We plot four cases namely $\beta = -0.333(3), -0.222(2), -0.11(1), -0.55(5)$ and we find the same behavior discussed in Fig. 5 though with different initial asymmetry. Notice that the model with $\beta = -0.555(5)$ does not give blue spectra but, nonetheless, it is driven towards isotropy for large positive times.

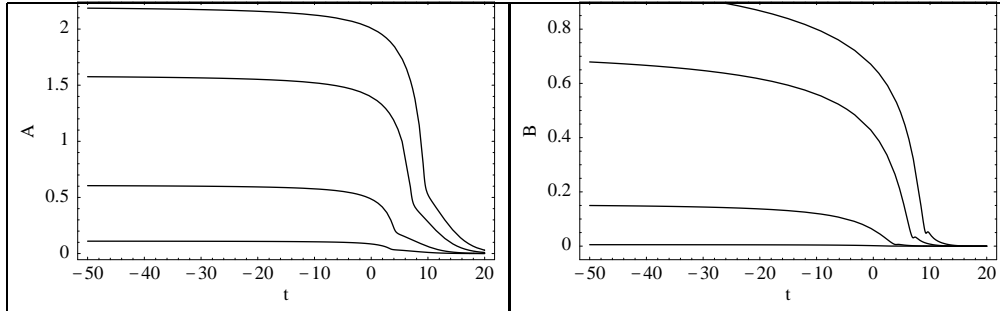


FIG. 6. Behavior of the asymmetries $A(t)$ and $B(t)$ for different initial conditions within the region of the (α, β) plane leading to blue axion spectra.

We recall that the motivation of this last section was to understand if string tension corrections can prevent the existence of anisotropic phases. In this sense, our conclusion is that string tension corrections do not prevent the existence of long anisotropic dilaton-driven epochs. Moreover, we showed that the models leading to blue axion spectra are likely to be attracted towards isotropic fixed points as a result of the string tension corrections.

VI. CONCLUDING REMARKS AND SPECULATIONS

In this paper we relaxed the isotropy assumption in the study of the amplification of the axionic fluctuations in string cosmology. In the isotropic case the four-dimensional spectra are typically red. We then focused our attention on the fully anisotropic (four-dimensional) dilaton driven solutions where the growing modes of the axion fluctuations are completely different from the one occurring in the completely isotropic case with the same number of dimensions. Assuming (as in the isotropic case) a smooth transition to a radiation dominated phase, the obtained axion spectra have an amplitude which depends upon the primordial anisotropy of the space-time encoded in the asymmetry between longitudinal and transverse momenta which can be expressed in terms of a primordial rapidity. The spectral slope is determined by the growing mode solution and can be either flat or blue for anisotropic models whose scale factors are all expanding though at a different rate. Our conclusions are summarized in Fig. 7.

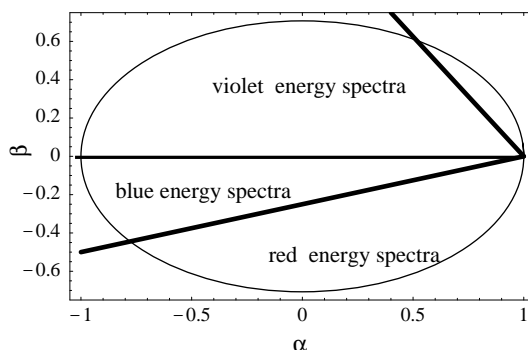


FIG. 7. Axionic logarithmic energy spectra for different dilaton-driven models with Kasner-like exponents (α, β) in the string frame.

As we showed the situation is qualitatively different if compared with the isotropic dilaton-driven evolution where only red spectra are possible. We focused our attention on blue spectra because they are produced by models with expanding four-volume and growing dilaton coupling. Red and violet spectra seem less natural from the anisotropic

point of view since they require that at least one of the scale factors contracts (in the string frame). We compared our phenomenological point of view with anisotropic models occurring as a result of spherically symmetric gravitational collapse and we showed that some of those models lead to blue axionic energy spectra. This conclusion extends and complements previous works on the subject [5,6].

Motivated by our phenomenological considerations we investigated the influence of string tension correction on the evolution of anisotropic dilaton-driven epochs. We found that string tension corrections never prevent the existence of anisotropic phases. Moreover if the anisotropy is mild (like in the region of Fig. 7 compatible with blue spectra) all the pre-big bang phase is anisotropic but it is attracted for large positive times towards an isotropic fixed point.

What we presented in this paper seem to suggest that it might be plausible to consider more seriously the possible effect of primordial anisotropies on the axionic spectra as it was recently done in the purely isotropic case [5]. It is not impossible to imagine that the amplitude of our spectra (and then the primordial ratio between longitudinal and transverse momenta) can be constrained by the temperature fluctuations in the Cosmic Microwave Background radiation. More generally, we find interesting that our considerations seem to point towards a more detailed analysis of anisotropic string cosmological models.

ACKNOWLEDGMENTS

I would like to thank G. Veneziano for very useful discussions.

APPENDIX A: MIXING COEFFICIENTS

In this appendix we report the mixing coefficients employed in the calculation of the energy spectrum of the amplified axionic perturbations discussed in Section III. Defining the function

$$S(r) = \frac{1}{\sqrt{r^2 + 1}}, \quad r = \frac{k_T}{k_L} \equiv \frac{\omega_T}{\omega_L} \quad (\text{A.1})$$

we have that the mixing coefficients are

$$\begin{aligned} c_-(k) &= \frac{[S(r)]^{5/2} \sqrt{x}}{2\sqrt{\pi}} e^{-ix[2+S(r)]} \left\{ (-3 - 4ix + \frac{2ix}{S(r)} - r^2(3 + 4ix)) U\left[\frac{3}{2} - \frac{i}{2}\epsilon r, 3, \frac{2ix}{S(r)}\right] \right. \\ &\quad \left. + \frac{2x}{S(r)} (3i + \epsilon r) U\left[\frac{5}{2} - \frac{i}{2}\epsilon r, 4, 2ixS(r)\right] \right\} \\ c_+(k) &= \frac{[S(r)]^{5/2} \sqrt{x}}{2\sqrt{\pi}} e^{-ix[2-S(r)]} \left\{ (-3 + 4ix + \frac{2ix}{S(r)} + r^2(-3 + 4ix)) U\left[\frac{3}{2} - \frac{i}{2}\epsilon r, 4, 2ixS(r)\right] \right. \\ &\quad \left. + \frac{2x}{S(r)} (3i + \epsilon r) U\left[\frac{5}{2} - \frac{i}{2}\epsilon r, 4, 2ixS(r)\right] \right\} \end{aligned} \quad (\text{A.2})$$

where $x = k\eta$.

APPENDIX B: EQUATIONS OF MOTION WITH STRING TENSION CORRECTIONS IN THE FULLY ANISOTROPIC CASE

Taking the variation of the action given in Eq. (5.6) with respect to the lapse function $N(t)$ and imposing, afterwards, the cosmic time gauge we get the constraint

$$\dot{\phi}^2 + 2\dot{\beta}^2 + 4\dot{\alpha}\dot{\beta} - 2\dot{\alpha}\dot{\phi} - 4\dot{\beta}\dot{\phi} + \left[\frac{3}{4}\dot{\phi}^4 - 6\dot{\alpha}\dot{\phi}\dot{\beta}^2 \right] = 0 \quad (\text{B.1})$$

where we took string units $\lambda_s = 1$ and $w = 1$. By varying the action with respect to α , β and ϕ we get, for $N(t) = 1$,

$$4\ddot{\beta} - 2\ddot{\phi} + (4\dot{\beta} - 2\dot{\phi})(\dot{\alpha} + 2\dot{\beta} - \dot{\phi}) - 2 \left[(\dot{\alpha} + 2\dot{\beta} - \dot{\phi})\dot{\phi}\dot{\beta}^2 + \ddot{\phi}\dot{\beta}^2 + 2\dot{\beta}\ddot{\beta}\dot{\phi} \right] + L(t) = 0, \quad (\text{B.2})$$

$$4(\ddot{\beta} + \ddot{\alpha} - \ddot{\phi}) + 4(\dot{\alpha} + \dot{\beta} - \dot{\phi})(\dot{\alpha} + 2\dot{\beta} - \dot{\phi}) - 4 \left[\ddot{\beta}\dot{\alpha}\dot{\phi} + \dot{\beta}\ddot{\alpha}\dot{\phi} + \dot{\beta}\dot{\alpha}\ddot{\phi} + \dot{\beta}\dot{\alpha}\dot{\phi}(\dot{\alpha} + 2\dot{\beta} - \dot{\phi}) \right] + 2L(t) = 0, \quad (\text{B.3})$$

$$\begin{aligned} &2(\ddot{\phi} - \ddot{\alpha} - 2\ddot{\beta}) + 2(\dot{\phi} - \dot{\alpha} - 2\dot{\beta})(\dot{\alpha} + 2\dot{\beta} - \dot{\phi}) \\ &- \left[2\dot{\beta}(\ddot{\alpha}\dot{\beta} + 2\dot{\alpha}\ddot{\beta}) + (2\dot{\alpha}\dot{\beta}^2 - \dot{\phi}^3)(\dot{\alpha} + 2\dot{\beta} - \dot{\phi}) - 3\dot{\phi}^2\ddot{\phi} \right] - L(t) = 0, \end{aligned} \quad (\text{B.4})$$

where we defined

$$L(t) = -\dot{\phi}^2 - 2\dot{\beta}^2 - 4\dot{\alpha}\dot{\beta} + 2\dot{\alpha}\dot{\phi} + 4\dot{\beta}\dot{\phi} + \frac{1}{4}(8\dot{\phi}\dot{\alpha}\dot{\beta}^2 - \dot{\phi}^4). \quad (\text{B.5})$$

Defining now

$$x(t) = \dot{\alpha}, \quad y(t) = \dot{\beta}, \quad z(t) = \dot{\phi} \quad (\text{B.6})$$

we get, after trivial algebra, the equations reported in Section VI.

In Section VI we also used an alternative measure of the anisotropy of a homogeneous space-time, namely the ratio between the Weyl and Riemann invariants. In the specific case of our metric this quantity reads:

$$B(t) = \frac{C_{\mu\nu\alpha\beta}C^{\mu\nu\alpha\beta}}{R_{\mu\nu\alpha\beta}R^{\mu\nu\alpha\beta}} \equiv \frac{1}{3} \frac{[xy - x^2 - \dot{x} + \dot{y}]^2}{[x^4 + 2x^2y^2 + 3y^4 + 2x^2\dot{x} + \dot{x}^2 + 4y^2\dot{y} + 2\dot{y}^2]} \quad (\text{B.7})$$

We can clearly see from the above expression that in the isotropic limit (i.e. $x = y$) $B(t) \rightarrow 0$, as expected.

-
- [1] G. Veneziano, *A Simple/Short introduction to Pre-Big- Bang Physics/Cosmology*, talk given at International School of Subnuclear Physics, 35th Course: Highlights: 50 Years Later, Erice, Italy, 26 Aug - 4 Sep 1997 (hep-th/9802057); G. Veneziano, Phys. Lett. B **265** (1991); M. Gasperini and G. Veneziano, Astropart. Phys. **1**, 317 (1993).
- [2] M. Gasperini and M. Giovannini, Phys. Rev. D **47**, 1519 (1993); R. Brustein, M. Gasperini, M. Giovannini, V. Mukhanov, and G. Veneziano, Phys. Rev. D **51**, 674 (1995); R. Brustein, M. Gasperini, M. Giovannini, and G. Veneziano, Phys. Lett. B **361**, 45 (1991); M. Giovannini, Phys. Rev. D **55**, 595 (1997).
- [3] M. Gasperini, M. Giovannini, and G. Veneziano, Phys. Rev. Lett. **75** 3796 (1995); D. Lemoine and M. Lemoine, Phys. Rev. D **52**, 1955 (1995); M. Giovannini, Phys. Rev. D **56**, 3198 (1997).
- [4] M. Gasperini, M. Giovannini, and G. Veneziano, Phys. Rev. D **52**, 6651 (1995); R. Durrer, M. Gasperini, M. Sakellariadou, and G. Veneziano, *Seeds of Large scale anisotropy in String Cosmology*, CERN-TH-98-069 gr-qc/9804076.
- [5] R. Durrer, M. Gasperini, M. Sakellariadou, and G. Veneziano, *Massless (Pseudo)scalar Seeds of CMB Anisotropy*, DFTT-27-98, astro-ph/9806015; M. Gasperini and G. Veneziano, *Constraints on Pre-Big-Bang Models for seeding Large Scale Anisotropy by Massive Kalb-Ramond Fields*, CERN-TH-98-180, hep-ph/9806327 .
- [6] E. J. Copeland, R. Easther and D. Wands, Phys. Rev. D **56**, 874 (1997).
- [7] G. Veneziano, Phys. Lett. B **406**, 297 (1997); J. Maharana, R. Onofri and G. Veneziano, JHEP **4**, 4 (1998); A. Buonanno, T. Damour, and G. Veneziano, *Pre-Big-Bang Bubbles from the Gravitational Instability of Generic String Vacua*, IHES-P-98-44, hep-th/9806230.
- [8] T. Perko, R. Matzner, and L. Shepley, Phys. Rev. D **6**, 969 (1972).
- [9] B. L. Hu, Phys. Rev. D **18**, 969 (1978).
- [10] M. Giovannini, Phys. Rev. D **57**, 7223 (1998); *Singularity free dilaton-driven cosmologies and pre-little-bangs*, DAMTP-1998-83, hep-th/9807049.
- [11] Ya. B. Zeldovich and A. A. Starobinsky, Zh. Eksp. Teor. Fiz. **61**, 2161 (1971) [Sov. Phys. JETP, **34**, 1159 (1971)]; A. G. Doroshkevich, V. N. Lukash, and I. D. Novikov, *ibid.* **64**, 1457 (1974) [Sov. Phys. JETP, **37** 739 (1973); V. N. Lukash and A. A. Starobinsky, *ibid.* **66**, 1515 (1974) [Sov. Phys. JETP **39**, 742 (1974)]; B. L. Hu and L. Parker, Phys. Rev. D **17**, 933 (1978); K. Jacobs, Astrophys. J. **153**, 661 (1968); K. Maeda, Phys. Rev. D **30**, 2482 (1984).
- [12] V. A. Belinskii and I. M. Khalatnikov, Zh. Eksp. Teor. Fiz. **57**, 2163 (1969) [Sov. Phys. JETP **30**, 1174 (1970); *ibid.* **63** 1121 (1972)[Sov. Phys. JETP **36**, 591 (1973)]; Usp. Fiz. Nauk. **102**, 463 (1970) [Sov. Phys. Usp. **13**, 745 (1971)].
- [13] M. Gasperini and G. Veneziano, Phys. Rev. D **50**, 2519 (1994); M. Gasperini, M. Giovannini, K. Meissner, and G. Veneziano, in *String theory in curved space times*, ed. N. Sanchez (World Scientific, Singapore, 1998), p. 49 (hep-th/9502130).
- [14] K. A. Meissner and G. Veneziano, Phys. Lett. B **267**, 33 (1997); Mod. Phys. Lett. A **6**, 3397 (1991); M. Gasperini, J. Maharana and G. Veneziano, Phys. Lett. B **272**, 277 (1991); M. Gasperini and G. Veneziano, Phys. Lett. B **277**, 256 (1992); K. A. Meissner *ibid.* **392**, 298 (1997); A. Sen, Phys. Lett. B **271**, 295 (1991); S. Hassan and A. Sen, Nucl. Phys. B **375**, 103 (1992).
- [15] M. Abramowitz and I. A. Stegun, *Handbook of mathematical functions* (Dover, New York, 1972).
- [16] L. D. Landau and E. M. Lifshitz, *Quantum Mechanics*, (Pergamon Press, London 1958).
- [17] P. S. Wesson, J. Math. Phys. **19**, 2283 (1978).
- [18] N. D. Birrel and P. C. Davies, *Quantum Fields in Curved Space*, (Cambridge Univesity Press, Cambridge, England, 1982).
- [19] M. Giovannini and M. Gasperini, Phys. Lett. B **301**, 334 (1993); M. Gasperini, M. Giovannini, and G. Veneziano, Phys. Rev. D **48**, 439 (1993); M. Gasperini and M. Giovannini, Class. Quantum Grav. **10** L133 (1993); M. Giovannini *Squeezed states and Gravitons-Entropy production in the Early Universe*, in Proc. of the “Third International Workshop on Squeezed States and Uncertainty Relations”, eds. W. Zachary and Y.S.Kim, NASA Conf. Publ. **3270**, 407 (1994).
- [20] Ya. B. Zeldovich and I. D. Novikov *The Structure and Evolution of the Universe*, Vol. 2 (Chicago University Press, Chicago 1971).
- [21] M. Gasperini, Phys. Rev. D **56**, 4815 (1997).
- [22] M. Gasperini, M. Maggiore, and G. Veneziano, Nucl. Phys. B **494**, 315 (1997); K. Meissner, Phys. Lett. B **392**, 298 (1997).
- [23] M. Gasperini and M. Giovannini, Phys. Lett. B **287**, 56 (1992); R. Brustein and G. Veneziano, Phys. Lett. B **329**, 429 (1994); I. Antoniadis, J. Rizos and K. Tamwakis, Nucl. Phys. B **415**, 497 (1993); R. Easther and K. Maeda, Phys. Rev. D **54**, 7252 (1996); R. Easther K. Maeda and D. Wands, Phys. Rev. D **53**, 4247 (1996).